



AALBORG UNIVERSITY
DENMARK

Aalborg Universitet

Wind turbine state estimation

Knudsen, Torben

Publication date:
2014

Document Version
Early version, also known as pre-print

[Link to publication from Aalborg University](#)

Citation for published version (APA):
Knudsen, T. (2014). Wind turbine state estimation.

General rights

Copyright and moral rights for the publications made accessible in the public portal are retained by the authors and/or other copyright owners and it is a condition of accessing publications that users recognise and abide by the legal requirements associated with these rights.

- ? Users may download and print one copy of any publication from the public portal for the purpose of private study or research.
- ? You may not further distribute the material or use it for any profit-making activity or commercial gain
- ? You may freely distribute the URL identifying the publication in the public portal ?

Take down policy

If you believe that this document breaches copyright please contact us at vbn@aub.aau.dk providing details, and we will remove access to the work immediately and investigate your claim.

Wind Turbine State Estimation

Torben Knudsen
Automation and Control
Department of Electronic Systems
Aalborg University

March 26, 2014



AALBORG UNIVERSITY
DENMARK

Abstract

Dynamic inflow is an effect which is normally not included in the models used for wind turbine control design. Therefore, potential improvement from including this effect exists. The objective in this project is to improve the methods previously developed for this and especially to verify the results using full-scale wind turbine data.

The previously developed methods were based on extended Kalman filtering. This method has several drawback compared to unscented Kalman filtering which has therefore been developed. The unscented Kalman filter was first tested on linear and non-linear test cases which was successful. Then the estimation of a wind turbine state including dynamic inflow was tested on a simulated NREL 5MW turbine was performed. This worked perfectly with wind speeds from low to nominal wind speed as the output prediction errors were white. In high wind where the pitch actuator was always active the results were not as convincing because the output prediction errors were not white. Using real data it has not been possible to get really good results so far. There remains a number of challenges: verifying turbine parameters and getting the most suitable measurement signals, including the 3P effect in the model and perhaps including the 1P effect. It is obviously difficult to make a final conclusion before the above challenges has been resolved.

Acknowledgement

This work has been funded by Norwegian Centre for Offshore Wind Energy (NORCOWE) under grant 193821/S60 from Research Council of Norway (RCN). NORCOWE is a consortium with partners from industry and science, hosted by Christian Michelsen Research. All the data necessary for the full scale experiments was kindly provided by Vestas Wind Systems A/S.

Contents

1	Introduction	4
1.1	Objectives	4
1.2	Approach and outline	4
2	Continuous discrete unscented Kalman filter	6
2.1	The continuous–discrete KF	6
2.2	The continuous–discrete EKF	7
2.3	Unscented transform	7
2.4	Unscented Kalman filter	11
2.5	Test of the UKF implementation	12
3	Dynamic inflow model	16
4	Test based on NREL 5MW simulations	17
4.1	Close to rated wind	17
4.2	High wind	17
4.3	Summary of results	17
5	Test based on full-scale data	23
5.1	First data	23
5.2	Second data sets	23
5.3	Low wind	24
5.4	Close to rated wind	26
5.5	Discussion	30
6	Conclusion	32

A	Measurement specifications	34
B	Parameter specifications	36
C	Second order statistics for $y = x^T x$ for x Gaussian	37
D	Detailed dynamic model	40

Chapter 1

Introduction

This report is part of the work done in the NORCOWE project by section for Automation and Control, Department for Electronic Systems, AAU. In the work plan for 2013 the following deliverable “Paper on methods for estimating the effective wind speed and available power at a single turbine.” is listed and covered by Knudsen and Bak [2013]. The results in this paper suggested new research especially using unscented instead of extended Kalman filtering and using a standard large commercial wind turbine instead of a small prototype for experimental verification. The results of this research is presented in this report.

1.1 Objectives

The significance of dynamic inflow is discussed in Knudsen and Bak [2013]. Especially for model based control design dynamic inflow could have an important role. The main objective in this project is to improve and verify the dynamic inflow model presented in Knudsen and Bak [2013]. Initially a second stage for 2014 was also discussed. This stage would include pursuing possible improvements for the inflow model. Moreover, data driven modelling of larger parts of the wind turbine model will be considered e.g. improving the C_p and C_t models. This report only covers the first stage.

1.2 Approach and outline

The original state estimator in Knudsen and Bak [2013] is based on a extended Kalman filter (EKF). EKF make use of a linearised state model. This makes it difficult to change the model as new partial derivatives have to be derived. The unscented Kalman filter (UKF) [Julier et al., 1995] uses the unscented transform [Thrun et al., 2006] to calculate necessary means and covariances and does not need linearization. Moreover, the UKF should have the same or better performance compared to the EKF depending on the type of non linearities. For these good reasons the EKF was exchanged with a UKF. In order to keep the parametrisation from the stochastic differential equations (SDE) from physics the EKF was of the continuous-discrete (CD) type i.e. based on the continuous SDE for the state and the discrete time measurement equation. Existing implementations of the UKF have only been found for the discrete-discrete (DD) case i.e. with discrete time state equation. Therefore a CD version of the UKF has been developed in section 2.4.

In Knudsen and Bak [2013] the drive train model is simply a one inertia model. As the drive train is only weakly damped drive train oscillations can occur depending on the controller. Therefore the drive train model used here consists of two masses one for the slow rotor part and one for the fast generator part, the two inertias are connected with a spring and damper. This extension and the rest of the model from Knudsen and Bak [2013] are briefly presented in section 3.

The developed UKF is tested on a “standard” non-linear system in section 2.4. One possible next step would be to directly test with full-scale data. An intermediate step taken here is to test the wind turbine state estimation on simulated data. This makes it possible to check for errors in the wind turbine specific part of the UKF implementation. When there are no more errors the results shows the performance for the simulated case which is assumed to be the the upper limit of what can be achieved with real data. The simulation test is presented in section 4.

Finally the UKF is tested on real full-scale data in section 5.

Chapter 2

Continuous discrete unscented Kalman filter

This section serves to document the ideas and understanding gained regarding UKF. This can appear rather technical and can be skipped for those who focus more on results.

For reference the basic KF filter for linear systems are first presented below.

2.1 The continuous–discrete KF

Assume the linear time varying system:

$$dx(t) = (F(t)x(t) + B(t)u(t)) dt + dw(t) \quad (2.1a)$$

$$y(t_k) = H(t_k)x(t_k) + D(t_k)u(t_k) + v(t_k) \quad (2.1b)$$

$$w(t) \in W(Q(t)), v(t_i) \in N(0, R(t_i)), E(v(t_i)v(t_j)^T) = \Delta(t_i - t_j)R(t_i) \quad (2.1c)$$

and the normal definitions

$$\hat{x}(t_k^-) \triangleq E(x(t_k)|Y_0^{t-1}), \quad (2.2a)$$

$$\hat{x}(t_k^+) \triangleq E(x(t_k)|Y_0^t), \quad (2.2b)$$

$$Y_0^t \triangleq y(t), y(t-1), \dots, y(0) \quad (2.2c)$$

$$P(t_k^-) \triangleq \text{Cov}(x(t_k)|Y_0^{t-1}) = E((x(t_k) - \hat{x}(t_k^-))(x(t_k) - \hat{x}(t_k^-))^T) \quad (2.2d)$$

$$P(t_k^+) \triangleq \text{Cov}(x(t_k)|Y_0^t) = E((x(t_k) - \hat{x}(t_k^+))(x(t_k) - \hat{x}(t_k^+))^T) \quad (2.2e)$$

Given measurements and initial values:

$$y(t_0), y(t_1), y(t_2) \dots, y(t), t \geq t_0, \quad (2.3a)$$

$$\hat{x}(t_0^-) = \hat{x}_0, P(t_0^-) = P_0 \quad (2.3b)$$

The KF can be formulated as follows:

Measurement update at time t_k :

$$K(t_k) = P(t_k^-)H(t_k)^T(H(t_k)P(t_k^-)H(t_k)^T + R(t_k))^{-1} \quad (2.4a)$$

$$\hat{x}(t_k^+) = \hat{x}(t_k^-) + K(t_k)(y(t_k) - H(t_k)\hat{x}(t_k^-) - D(t_k)u(t_k)) \quad (2.4b)$$

$$P(t_k^+) = (I - K(t_k)H(t_k))P(t_k^-)(I - K(t_k)H(t_k))^T + K(t_k)R(t_k)K(t_k)^T \quad (2.4c)$$

Time update from t_k to t_{k+1} :

$$\hat{x}(t_k) = \hat{x}(t_k^+), \quad P(t_k) = P(t_k^+) \quad (\text{initial conditions}) \quad (2.5a)$$

$$\dot{\hat{x}}(t) = F(t)\hat{x}(t) + B(t)u(t) \quad (\text{diff. eq. for } \hat{x}) \quad (2.5b)$$

$$\dot{P}(t) = F(t)P(t) + P(t)F(t)^T + Q(t) \quad (\text{diff. eq. for } P) \quad (2.5c)$$

$$\hat{x}(t_{k+1}^-) = \hat{x}(t_{k+1}), \quad P(t_{k+1}^-) = P(t_{k+1}) \quad (\text{Result}) \quad (2.5d)$$

2.2 The continuous–discrete EKF

Assume now the nonlinear model (2.6).

$$dx(t) = f(x(t), u(t))dt + dw(t) \quad (2.6a)$$

$$y(t_k) = h(x(t_k), u(t_k)) + v(t_k) \quad (2.6b)$$

The extended EKF is then derived from the KF by using the following heuristic principle: use the nonlinear relations when possible and the linearization otherwise.

This means that the following are changed to use the nonlinear equations.

Measurement update at time t_k :

$$\hat{x}(t_k^+) = \hat{x}(t_k^-) + K(t_k)(y(t_k) - h(\hat{x}(t_k^-), u(t_k), t_k)) \quad (2.7)$$

Time update from t_k to t_{k+1} :

$$\dot{\hat{x}}(t) = f(\hat{x}(t), u(t), t) \quad (\text{diff. eq. for } \hat{x}) \quad (2.8)$$

In all the other equations the linearized parameters (2.9) must be used.

$$F(x, u, t) \triangleq \frac{\partial f(x, u, t)}{\partial x} \quad (2.9a)$$

$$H(x, u, t) \triangleq \frac{\partial h(x, u, t)}{\partial x} \quad (2.9b)$$

It is best to use the most recent values of the state estimate, i.e.,

$$H(t_k) = H(t_k, \hat{x}(t_k^-), u(t_k^-)) \quad (2.10)$$

$$F(t) = F(t, \hat{x}(t|t_k), u(t)) \quad (2.11)$$

2.3 Unscented transform

The basic new idea in the UKF is to use the unscented transform (UT) to calculate necessary conditional means and covariances in the measurement (2.4) and time update (2.5). The problem solved by the UT is

the basic probabilistic problem of calculating the statistics of x, y given the statistics of x and a relation f :

$$y = f(x), \mu_x = E(x), C_x = \text{Cov}(x) \quad (2.12)$$

For non-linear relations there is no exact solution to find even the second order statistics. The EKF can be interpreted as using the linearization approach:

$$y \sim f(\mu_x) + \nabla f(\mu_x)(x - f(\mu_x)) \Rightarrow \quad (2.13)$$

$$\mu_y = f(\mu_x), C_{yx} = \nabla f(\mu_x)C_x, C_y = \nabla f(\mu_x)C_x \nabla f(\mu_x)^T \quad (2.14)$$

A Monte Carlo approach would be to generate random realisations x_i based on the statistics for x and estimating the statistics for x, y as follows:

$$\hat{\mu}_y = \frac{1}{N} \sum_{i=1}^N f(x_i), \hat{\mu}_x = \frac{1}{N} \sum_{i=1}^N x_i, \quad (2.15)$$

$$\hat{C}_{yx} = \frac{1}{N} \sum_{i=1}^N (f(x_i) - \hat{\mu}_y)(x_i - \hat{\mu}_x)^T, \hat{C}_y = \frac{1}{N} \sum_{i=1}^N (f(x_i) - \hat{\mu}_y)(f(x_i) - \hat{\mu}_y)^T, \quad (2.16)$$

The UT can be seen as the Monte Carlo method but where the x_i 's are not randomly drawn but constructed to obtain certain features these constructed x_i 's are called sigma points. Especially if x is Gaussian it is natural to use the eigen vectors of C_x to construct the sigma points. The UT used here is given below where n is the dimension of x .

$$\alpha = 1, \kappa = 2, \beta = 0, \text{ (Default parameters gives } \lambda = 2) \quad (2.17a)$$

$$\lambda = \alpha^2(n + \kappa) - n, \quad (2.17b)$$

$$k = \sqrt{n + \lambda}, \quad (2.17c)$$

$$u_i \triangleq \text{eigenvector } i \text{ for } C_x, l_i \triangleq \text{eigenvalue } i \text{ for } C_x, \quad (2.17d)$$

$$x_i = \begin{cases} \mu_x & , i = 0 \\ \mu_x + k u_i \sqrt{l_i} & , 1 \leq i \leq n \\ \mu_x - k u_i \sqrt{l_i} & , n + 1 \leq i \leq 2n \end{cases} \quad (2.17e)$$

$$w_i^t = \begin{cases} \frac{\lambda}{n + \lambda} & , i = 0, t = m \text{ (for mean)} \\ \frac{\lambda}{n + \lambda} + 1 - \alpha^2 + \beta & , i = 0, t = c \text{ (for covarians)} \\ \frac{1}{2(n + \lambda)} & , 1 \leq i \leq 2n \end{cases} \quad (2.17f)$$

$$\hat{\mu}_y = \sum_{i=0}^{2n} w_i^m f(x_i), \quad (2.17g)$$

$$\hat{C}_{yx} = \sum_{i=0}^{2n} w_i^c (f(x_i) - \hat{\mu}_y)(x_i - \hat{\mu}_x)^T, \quad (2.17h)$$

$$\hat{C}_y = \sum_{i=0}^{2n} w_i^c (f(x_i) - \hat{\mu}_y)(f(x_i) - \hat{\mu}_y)^T, \quad (2.17i)$$

Notice that $\sum_{i=0}^{2n} w_i^m = 1$ and for the chosen parameters $w_i^m = w_i^c$. This construction can be shown to give exactly correct results for linear and affine functions $f(x) = Ax + b$. Here eigen vectors are used to

construct the sigma points. There are other ways, e.g. Cholesky factorisation, which gives correct results for linear functions but different results for non-linear functions.

The above UT has been tested and compared to both the MC method and the version using Cholesky factorisation. A number of different functions $f(x)$ has been tested. In general the two versions of the UT transform are quit similar. In order to have a test where the correct result is known the $E(y)$ and $Cov(y, x)$ is derived in appendix C for $y = x^T x$. The results are shown in figure 2.1– 2.3 and table 2.1 for the Gaussian case with $E(x) = [1; 1]$ and $Cov(x) = [1 \ 1; 1 \ 2]$ (using Matlab notation).

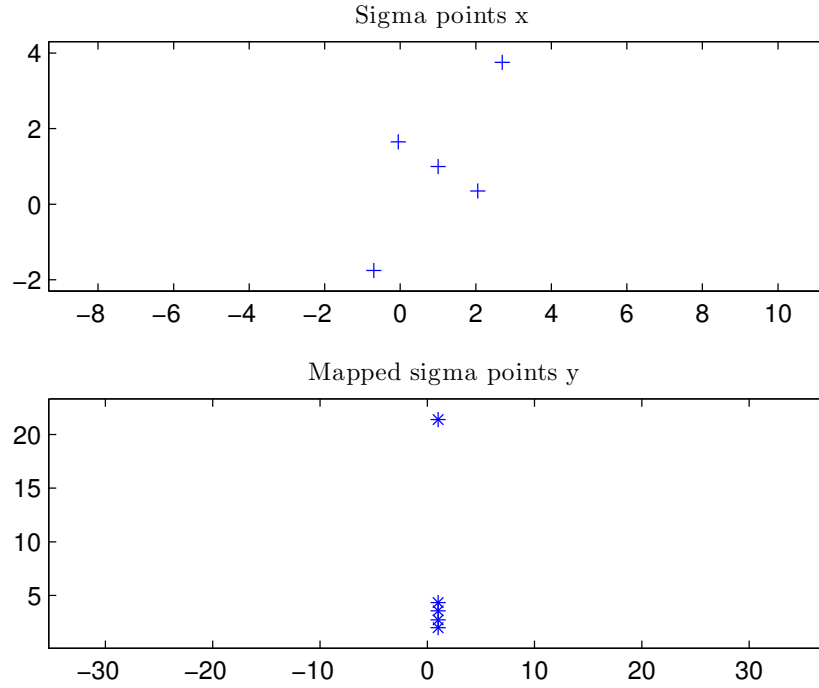


Figure 2.1: Sigma points and images for the UT based on (2.17).

Method	My	Cy	Cyx	
UTSCEst	5.000e+00	3.900e+01	4.000e+00	6.000e+00
UTJMEst	5.000e+00	3.100e+01	4.000e+00	6.000e+00
UTMCEst	5.038e+00	3.385e+01	3.988e+00	6.028e+00
THTK	5.000e+00	3.400e+01	4.000e+00	6.000e+00
UTSCRelE	0	1.471e-01	0	0
UTJMRelE	0	-8.824e-02	0	0
UTMCRelE	7.663e-03	-4.284e-03	-3.090e-03	4.670e-03

Table 2.1: Performance for the above method, the Cholesky based, the MC and the theoretical. The rows marked RelE are the errors relative to the correct results.

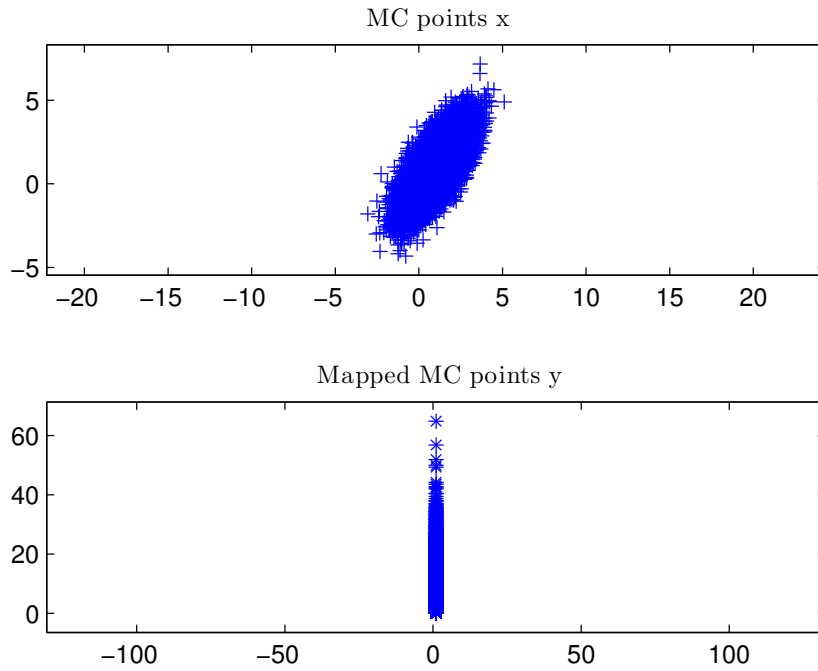


Figure 2.2: Sigma points and images for the MC based method.

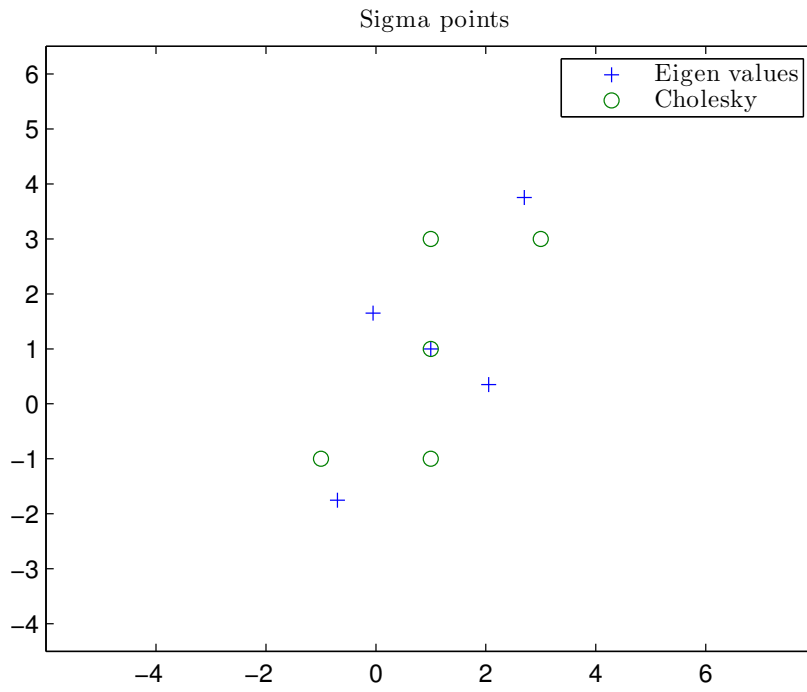


Figure 2.3: Comparison of sigma points based on eigenvalues and the Cholesky method.

2.4 Unscented Kalman filter

To understand the UKF it is necessary to follow the derivation of the KF to recognise that the measurement update (2.4b) and (2.4c) originates from basic relation for Gaussian variables. Assume x, y are Gaussian vectors then the least mean square (LMS) error estimate for x given y is the conditional mean $E(x|y)$.

$$E(x|y) = E(x) + \text{Cov}(x, y) \text{Cov}(y)^{-1} (y - E(y)) , \quad (2.18a)$$

$$\text{Cov}(x|y) = \text{Cov}(x) - \text{Cov}(x, y) \text{Cov}(y)^{-1} \text{Cov}(y, x) , \quad (2.18b)$$

where

$$\text{Cov}(x, y) \triangleq E((x - E(x))(y - E(y))^T) , \quad (2.18c)$$

$$\text{Cov}(x) \triangleq \text{Cov}(x, x) \quad (2.18d)$$

If some information z is already available and some new information y will be obtained the similar formulas are

$$E(x|y, z) = E(x|z) + \text{Cov}(x, y|z) \text{Cov}(y|z)^{-1} (y - E(y|z)) , \quad (2.19a)$$

$$\text{Cov}(x|y, z) = \text{Cov}(x|z) - \text{Cov}(x, y|z) \text{Cov}(y|z)^{-1} \text{Cov}(y, x|z) \quad (2.19b)$$

Applying this where x, y, z are $x(t_k), \tilde{y}(t_k^-), Y_0^{t-1}$ gives the following

$$\hat{x}(t_k^+) = \hat{x}(t_k^-) + \text{Cov}(\tilde{x}(t_k^-), \tilde{y}(t_k^-)) \text{Cov}(\tilde{y}(t_k^-))^{-1} \tilde{y}(t_k^-) , \quad (2.20a)$$

$$P(t_k^+) = P(t_k^-) - \text{Cov}(\tilde{x}(t_k^-), \tilde{y}(t_k^-)) \text{Cov}(\tilde{y}(t_k^-))^{-1} \text{Cov}(\tilde{y}(t_k^-), \tilde{x}(t_k^-)) , \quad (2.20b)$$

$$\tilde{y}(t_k^-) \triangleq y(t_k) - E(y(t_k)|Y_0^{t-1}) = y(t_k) - H(t_k)\hat{x}(t_k^-) - D(t_k)u(t_k) , \quad (2.20c)$$

$$\tilde{x}(t_k^-) \triangleq x(t_k) - E(x(t_k)|Y_0^{t-1}) , \quad (2.20d)$$

$$\text{Cov}(x(t_k), \tilde{y}(t_k^-)|Y_0^{t-1}) = \text{Cov}(\tilde{x}(t_k^-), \tilde{y}(t_k^-)) , \quad (2.20e)$$

$$\text{Cov}(\tilde{y}(t_k^-)|Y_0^{t-1}) = \text{Cov}(\tilde{y}(t_k^-)) \quad (2.20f)$$

this can be verified in the linear case using:

$$K(t_k) = \text{Cov}(\tilde{x}(t_k^-), \tilde{y}(t_k^-)) \text{Cov}(\tilde{y}(t_k^-))^{-1} , \quad (2.21a)$$

$$\text{Cov}(\tilde{y}(t_k^-)) = H(t_k)P(t_k^-)H(t_k)^T + R(t_k) \quad (2.21b)$$

The UKF measurement update, corresponding to (2.4b)–(2.4c) in the linear case, are given by (2.20a)–(2.20b) where the UT for the measurement equation

$$y(t_k) = h(x, u) + v = h_a([x, v], u) \quad (2.22)$$

with the input statistics

$$E \begin{pmatrix} x \\ v \end{pmatrix} = \begin{pmatrix} \hat{x}(t_k^-) \\ \underline{0} \end{pmatrix} , \quad (2.23)$$

$$\text{Cov} \begin{pmatrix} x \\ v \end{pmatrix} = \begin{pmatrix} P(t_k^-) & \underline{0} \\ \underline{0} & R(t_k) \end{pmatrix} \quad (2.24)$$

gives the output-input statistics

$$\hat{y}(t_k^-), \text{Cov}(\tilde{y}(t_k^-), \tilde{x}(t_k^-)) = \text{Cov}(\tilde{x}(t_k^-), \tilde{y}(t_k^-))^T, \text{Cov}(\tilde{y}(t_k^-)) \quad (2.25)$$

which are necessary in the UKF measurement update (2.20a)–(2.20b).

The UKF time update using UT calls for a function definition of this step. From a mathematical point of view the input to this function is $\hat{x}(t_k^-), P(t_k^-), u(t), t \in [t_k, t_{k+1}], Q(t), t \in [t_k, t_{k+1}]$. The first two inputs comes from the measurement update step just explained and the two last inputs are assumed known. The output of the function must be the result of integrating the state SDE (2.26) from t_k to t_{k+1} .

$$dx(t) = f(x(t), u(t))dt + dw(t) \quad (2.26)$$

As w is a Wiener process it has independent increments with variance $V(w(t + \delta t) - w(t)) = Q(t)\delta t$. This can be approximated using Runge-Kutta (RK4) integration of the difference equation

$$\delta x(t) = f(x(t), u(t))\delta t + \delta w(t) \quad (2.27)$$

$$\delta x(t) = (f(x(t), u(t)) + \delta w(t)/\delta t)\delta t \quad (2.28)$$

$$\delta x(t) = (f(x(t), u(t)) + \delta w(t)/\delta t)\delta t \quad (2.29)$$

$$\delta x(t) = (f(x(t), u(t)) + n(t))\delta t \quad (2.30)$$

$n(t)$ should then be a process with independent increments and variance $Q(t)(\delta t)^{-1}$. If the (RK4) integration has n_i intermediate steps the final state

$$x_f(t_{k+1}) = f_a([x_i(t_k), N_{t_k}^{t_{k+1}}, U_{t_k}^{t_{k+1}}]) \quad (2.31)$$

will be a function of the initial state and stacked noise N and input U for the intermediate time steps in the integration and the UT transform can be used with the input statistics

$$\text{E} \begin{pmatrix} x_i \\ N \end{pmatrix} = \begin{pmatrix} \hat{x}(t_k^-) \\ \underline{0} \\ \vdots \\ \underline{0} \end{pmatrix}, \quad (2.32)$$

$$\text{Cov} \begin{pmatrix} x_i \\ N \end{pmatrix} = \begin{pmatrix} P(t_k^-) & \underline{0} & \dots & \underline{0} \\ \underline{0} & Q(t_k)/\delta t & \dots & \underline{0} \\ \underline{0} & \dots & \ddots & \underline{0} \\ \underline{0} & \dots & \dots & Q(t_{k+1})/\delta t \end{pmatrix} \quad (2.33)$$

gives the output-input statistics

$$\hat{x}(t_{k+1}^-), P(t_{k+1}^-) = \text{Cov}(\tilde{x}(t_{k+1}^-)) \quad (2.34)$$

which are necessary in the UKF time update corresponding to (2.5).

As seen above the UKF can be interpreted as using the UT to calculate the conditional means, variances and covariances necessary in the KF.

2.5 Test of the UKF implementation

The UKF described above has been turned into a MATLAB program. A DD version has also been made and then, from previous development, we have both EKF and KF also in both a DD and CD version.

To test the CD UKF developed above a number of simulations of SDE has been done. Simulation with linear SDE's shows that all KF versions behaves as expected and produces white residuals. This just serves to rule out programming errors. Two non-linear SDE has also been tested. One with polynomial non-linearities and a Lorenz system with noise. In all cases the CD UKF performed at least as well as the other KF measured by state prediction error RMS and output prediction error whiteness. In many cases CD UKF was very superior. There were also cases where the CD UKF was much better than the DD UKF even though only one step in the RK4 integration was used.

Below some results from the Lorenz SDE (2.35) are shown.

$$dx = f(x)dt + dw , \quad (2.35a)$$

$$y = x + v , \quad (2.35b)$$

$$f(x) = \begin{pmatrix} \sigma(x_2 - x_1) \\ x_1(\rho - x_3) - x_2 \\ x_1x_2 - \beta x_3 \end{pmatrix} , \quad (2.35c)$$

$$w \in W(0, Q) , \quad (2.35d)$$

$$v \in \text{NID}(0, R) , \quad (2.35e)$$

$$\sigma = 10 , \rho = 8 , \beta = 8/3 , Q = 0.1^2 I , R = I , T_s = 0.01 , x(0) = (-1 \ 3 \ 4)^T \quad (2.35f)$$

As seen in figure 2.4– 2.7 the results are good as everything is as expected e.g. white noise test is OK

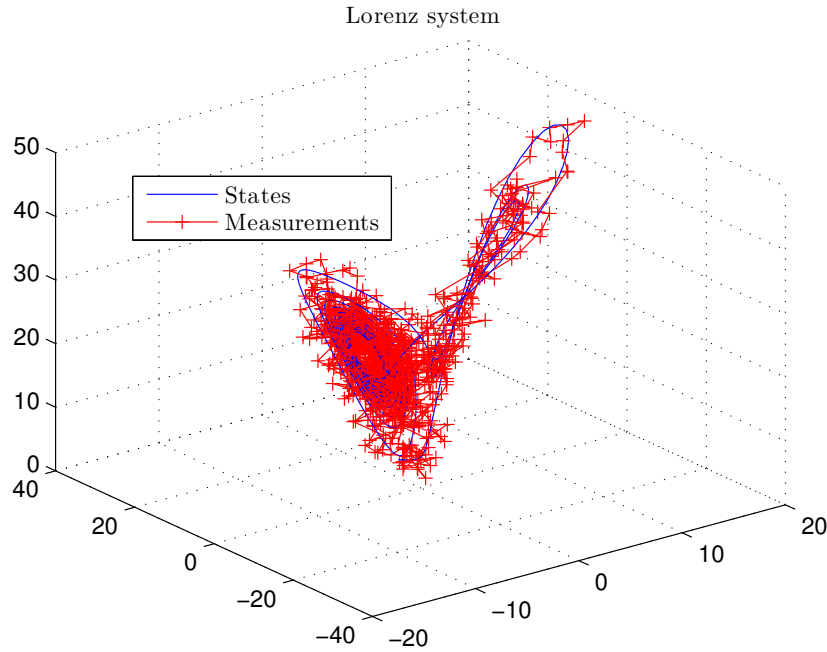


Figure 2.4: Simulated states and measurements for the Lorenz system.

and also the rms on state prediction errors is close to the average covariances calculated by the UKF. For the three states the fraction between rms and calculated covariances are 0.95, 0.94, 1.06 respectively.

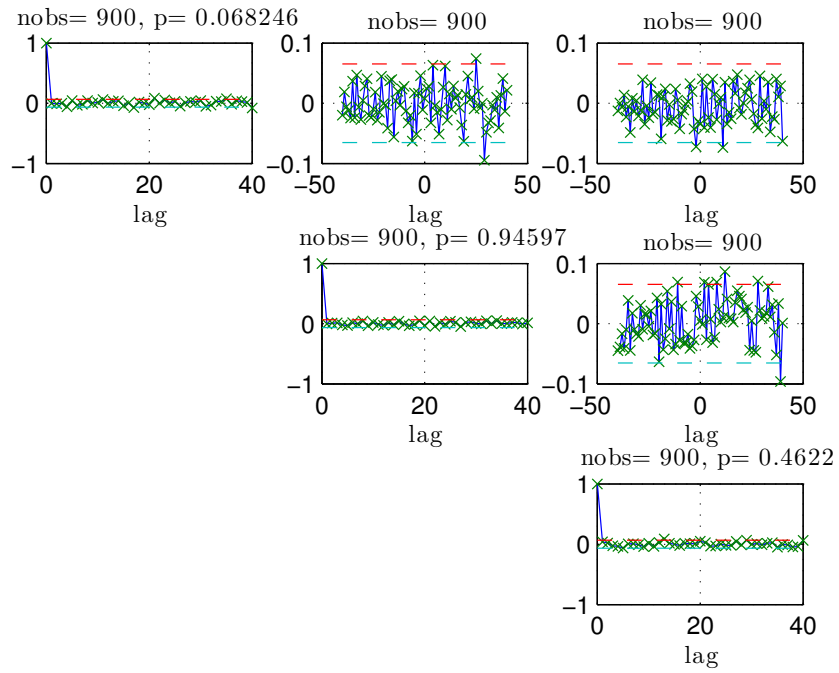


Figure 2.5: Whiteness test for residuals.

Residuals with 2 standard deviations error bounds

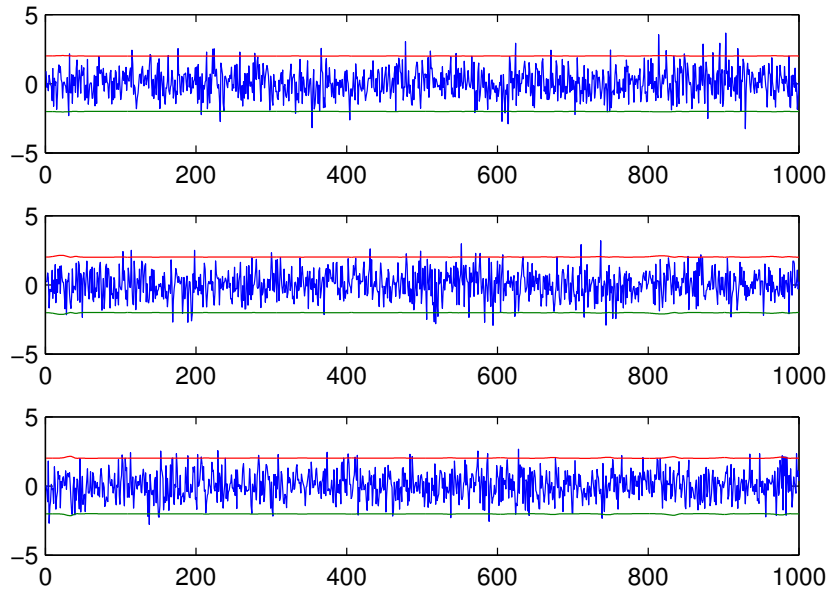


Figure 2.6: Output prediction errors (residuals) vs time including 0.95 confidence limits.

State prediction errors with 2 standard deviations error bounds

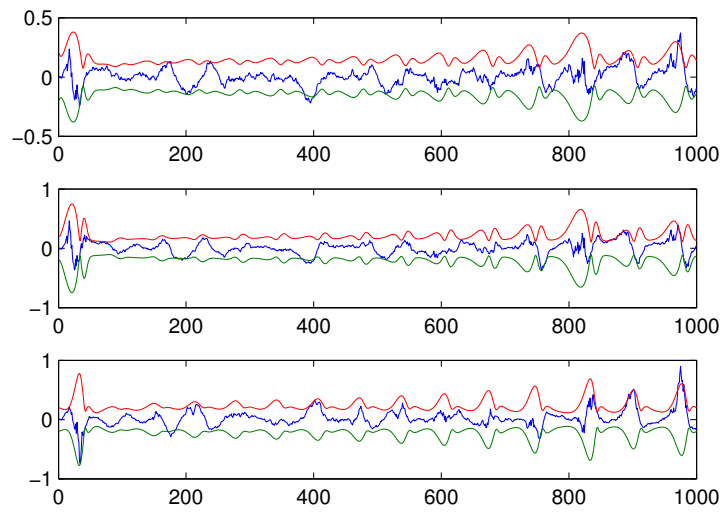


Figure 2.7: State prediction errors (residuals) vs time including 0.95 confidence limits.

Chapter 3

Dynamic inflow model

To use the UKF for estimating wind turbine states, a state and measurement equation corresponding to (2.6), is needed. The model is an extension of the one used in Knudsen and Bak [2013]. It is explained in general terms in this section. The mathematical details can be found in Knudsen and Bak [2013] and in appendix D where the extension is included.

The dynamic part of the model can be split into disturbance i.e. wind flow, input actuators, control subject i.e. mechanics and output part. The ambient wind speed is modelled as a mean part which is integrated white noise plus the turbulence which has a Kaimal spectrum. The dynamic inflow is modelled via an induction factor which is a first order filtering of the static induction factor. The inputs are measured pitch and generator torque and not their reference values so there is no reason to include input dynamics also the noise on the inputs are assumed negligible. The mechanics is modelled with a 2 DOF drive train and a 1 DOF tower fore-aft model. In the original model in Knudsen and Bak [2013] only one DOF (inertia) was used for the drive train. The outputs consist of generator speed, nacelle wind speed and nacelle fore AFT acceleration all with noise but no dynamics. Notice that 1P and 3P disturbances in the measurements are not considered. For simulation all the parameters are obtained from the model. For full-scale most of the parameters are obtained from the manufacturer while the rest, e.g. for the noise part, are guessed and estimated.

Chapter 4

Test based on NREL 5MW simulations

In advance it is not known how well the UKF performs or if it works at all. The theoretical optimal known performance for KF estimators only applies to linear systems. For non-linear systems we can only hope for good performance. For this reason the UKF will be tested using simulated data to see the performance under ideal conditions.

For this a Simulink implementation of the model in section 3 has been used. Notice that the model and system is then the same. The challenge for the UKF is then the non-linearities not any unmodeled dynamics.

There are some differences in performance depending on the mean wind speed. Therefore examples of rated (medium) and high wind speed are shown below.

4.1 Close to rated wind

At mean wind speed 11 m/s the pitch is not always active as seen in figure 4.1. For this situation the UKF performs as for a linear system so state predictions stays within calculated confidence intervals as show for the induction in figure 4.3 and all residuals are white as seen in figure 4.4.

4.2 High wind

In high winds where the pitch is mostly active the performance is not that close to ideal as seen for mean wind speed 15 m/s in figure 4.5–4.8.

4.3 Summary of results

The results in section 4.1– 4.2 are examples of the general picture shown in table 4.1. Here it is clearly seen that the performance of the UKF depart more from the ideal as the pitch activity, and the mean wind, increases.

There is to possible causes for this disappointing performance:

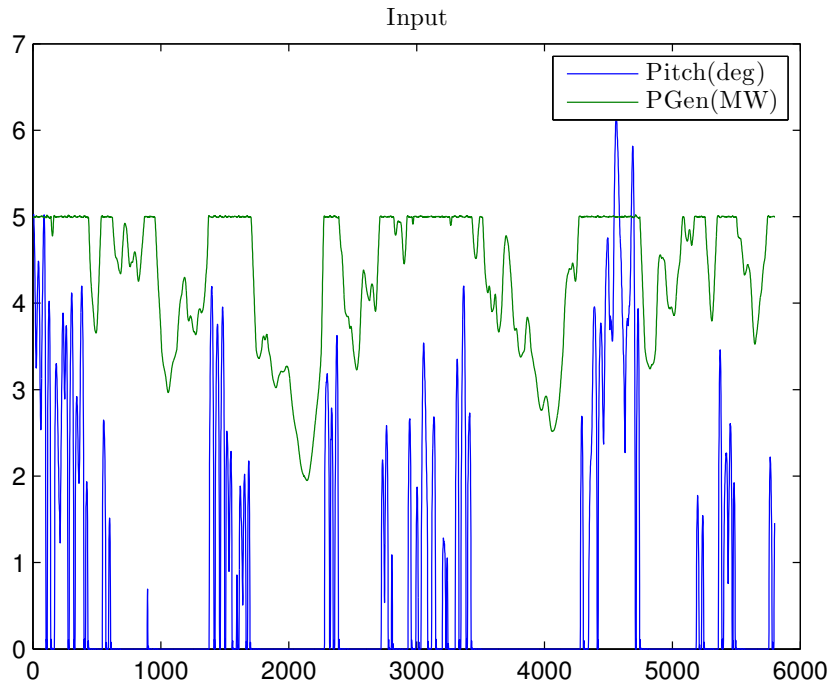


Figure 4.1: Input for the NREL 5MW simulated test at mean wind 11m/s.

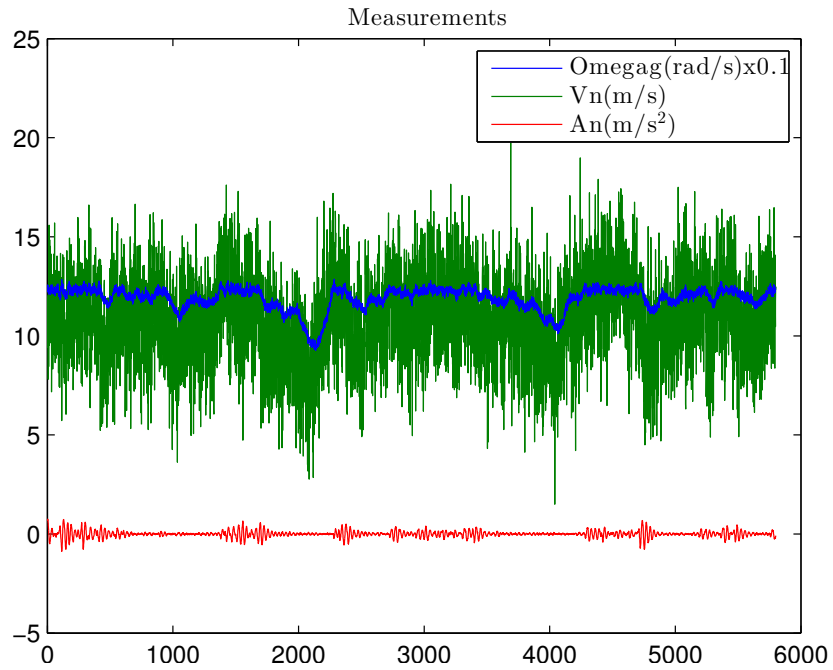


Figure 4.2: Measurements for the NREL 5MW simulated test at mean wind 11m/s.

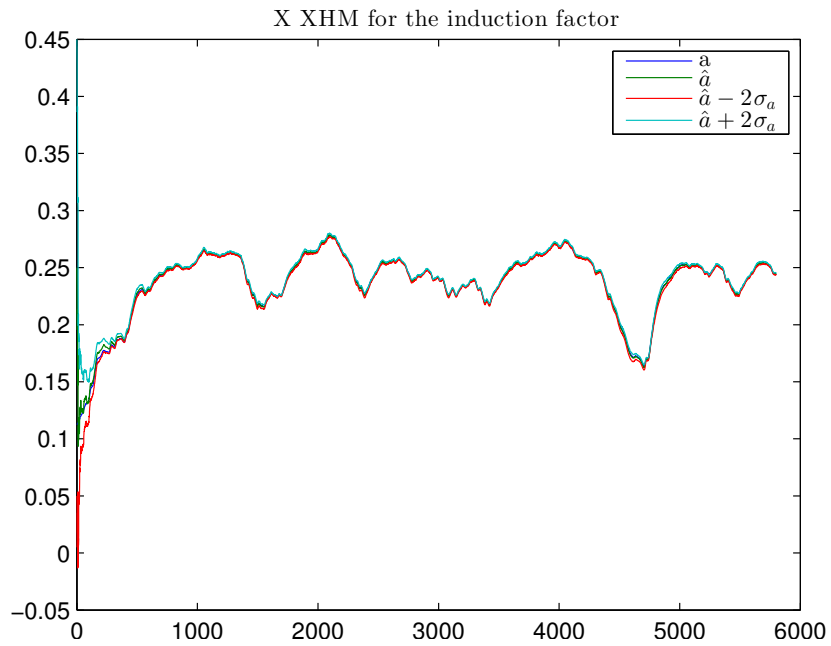


Figure 4.3: Induction factor and confidence limits for the NREL 5MW simulated test at mean wind 11m/s.

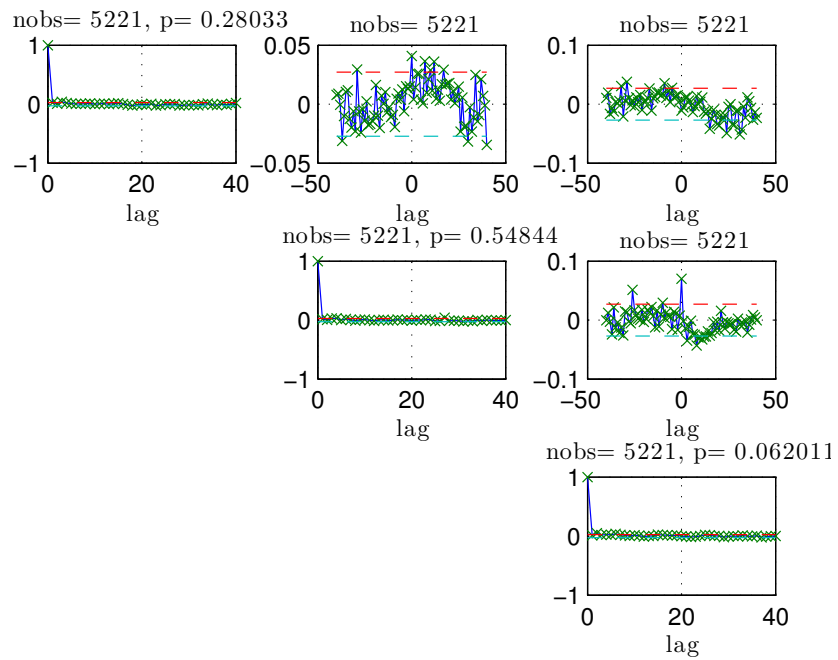


Figure 4.4: Residual test for the NREL 5MW simulated test at mean wind 11m/s.

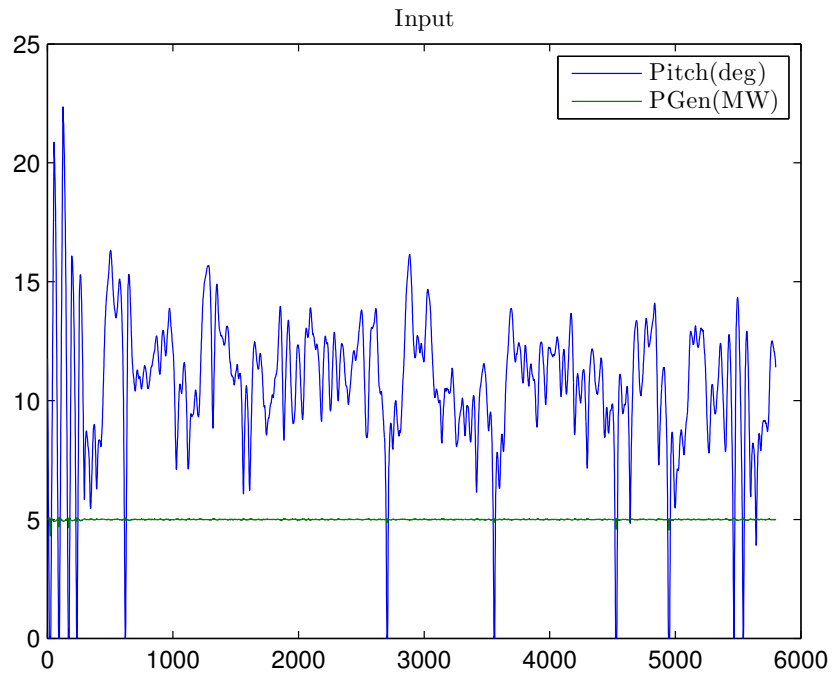


Figure 4.5: Input for the NREL 5MW simulated test at mean wind 15m/s.

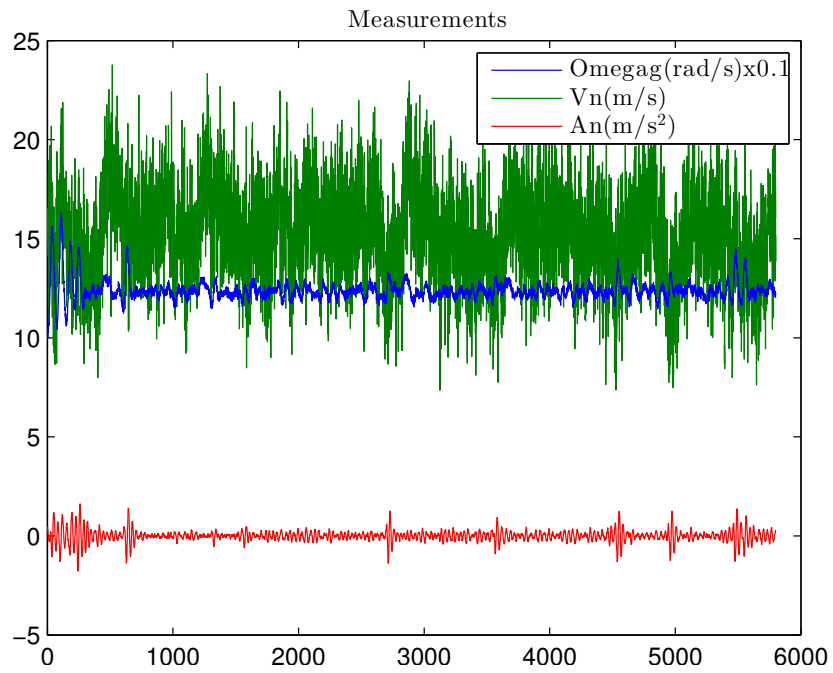


Figure 4.6: Measurements for the NREL 5MW simulated test at mean wind 15m/s.

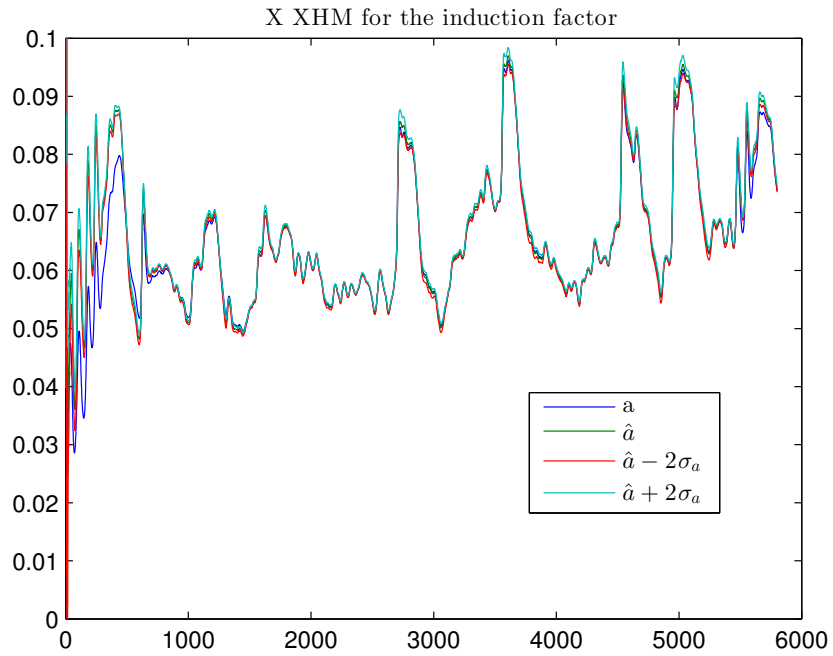


Figure 4.7: Induction factor and confidence limits for the NREL 5MW simulated test at mean wind 15m/s.

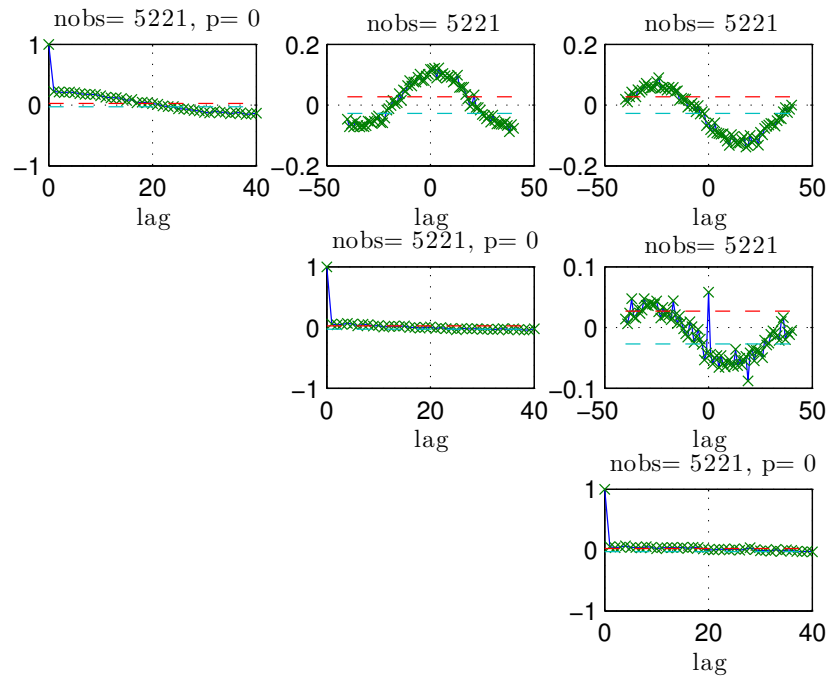


Figure 4.8: Residual test for the NREL 5MW simulated test at mean wind 15m/s.

Mean wind	Pitch > 0.1	Min p	Max corr.	Observed state rms/ estimated std
7	0	0.18		1.08
9	0.002	0.66		1.21
11	0.29	0.06		1.50
13	0.94	0.00	0.16	3.22
15	0.99	0.00	0.22	3.28
20	0.996	0.00	0.23	5.52

Table 4.1: Summary results by mean wind speed. Min p is the minimal p value in the Portmanteau test, Max corr. is the maximum estimated auto correlation between lag 1 and 40.

- The non-linearities are to large.
- The observability are to low when the pitch feedback is mostly active.

It has not been possible to find the cause so far.

Chapter 5

Test based on full-scale data

In this section the full-scale data are first discussed and then the estimation results are presented.

The data and parameter specification follows from the model in section 3 and appendix D and is therefore placed in appendix A– B.

5.1 First data

The first data was from a special test of something else. This is data sampled at 100 Hz. The pitch steps are every 15 sec. i.e. with a period of 30 sec. The mean wind speed is very low at 4.7 m/s.

The signals never reaches aerodynamic stationarity because the pitch changes every 15 sec. are too fast compared to the assumed time constant for dynamics inflow at $3D/2V$ i.e. approximately 36 sec. So the step is only half the time constant not the double which would be better. The very low wind speed is also a disadvantage as the effect of dynamic inflow is most pronounced close to rated power. Consequently these data have not been further used.

5.2 Second data sets

A second collection of data was kindly provided by the turbine manufacturer. These data was sampled with 10 Hz, had a duration from 300–600 sec., a average power from 0.33–0.93 of rated power and from 1–3 pitch “steps”. So far this seems promising.

After testing the estimation method with several of the data sets the results suggested that the tower eigen frequency might be wrong. The manufacturer corrected the frequency to 0.69 of the initial value and also corrected the structural damping which is anyway low compared to the aerodynamic damping.

With the new lower tower frequency the fraction between this and the 1P frequency is only 1.09 at rated speed. Especially with just a little over speeding the 1P can easily affect the tower. This was not expected as these frequencies should be separated. Further it is a problem because the 1P and 3P effects are not included in the model.

The nacelle wind speed included in the measurement is the direct reading by the anemometer corrected in

a way that should make it represent the corresponding ambient wind speed. For the estimation purpose the direct wind speed reading is the best as it carries information about the induction. Alternatively the correction procedure used could perhaps be used to map the corrected value back to the original. Unfortunately, neither of these requests were solved by the manufacturer.

5.3 Low wind

The “tuning” parameters for the KF is the process noise incremental covariance and the measurement covariance. The process noise consists of turbulence and “average” (10 min.) wind speeds. The wind parameters are fixed with turbulence intensity at 0.1 and the length scale parameter L at 170.1. The “average” wind speed is modelled as integrated white noise with incremental covariance $2^2/600$ i.e. a variance increase of 2^2 in 600 sec. The process noise parameters above are mostly based on physical considerations. The measurement noise parameters are based on experience, judgement and information from the manufacturer. The measurement noise covariance is diagonal with elements corresponding to the standard deviations $0.001\omega_{g,n}$, $2[m/s]$, $0.1[m/s^2]$.

The first data set last for 600 sec. The input in figure 5.1 shows the 3 pitch steps included which gives some nacelle movement as seen in figure 5.2. An example of the state estimates is shown in figure 5.3 where the estimated induction factor is plotted. In contrast to the simulation study in section 4 it is not possible to show the right induction factor here. However, it is possible to do the test for white

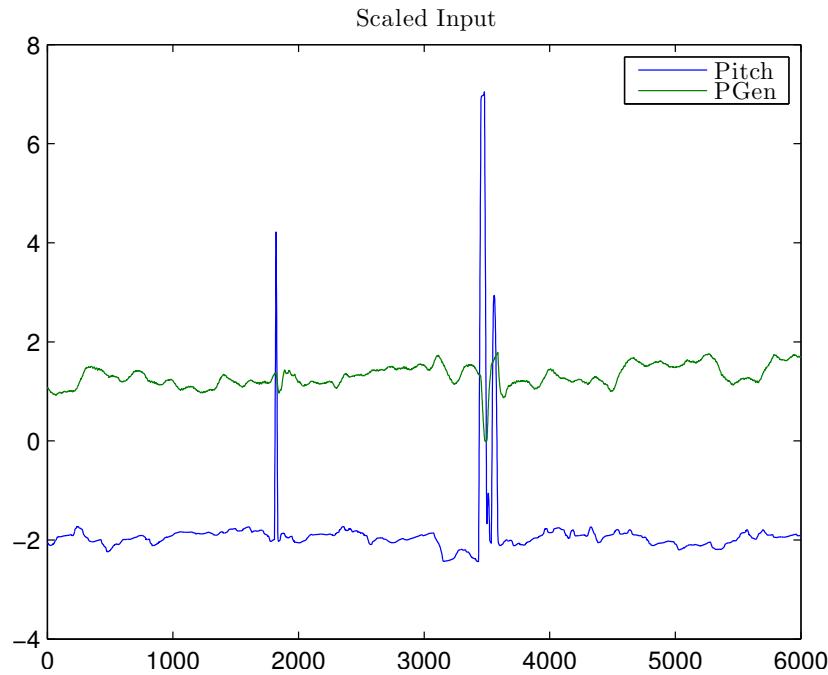


Figure 5.1: Input for full-scale test at mean wind below rated.

residuals as seen in figure 5.4. These are not white at all. To identify the frequencies the spectra for these residuals are shown in figure 5.5. The wind measurements residual is mostly of low pass type maybe because of some signal filtering which is not specified by the manufacturer. The generator speed

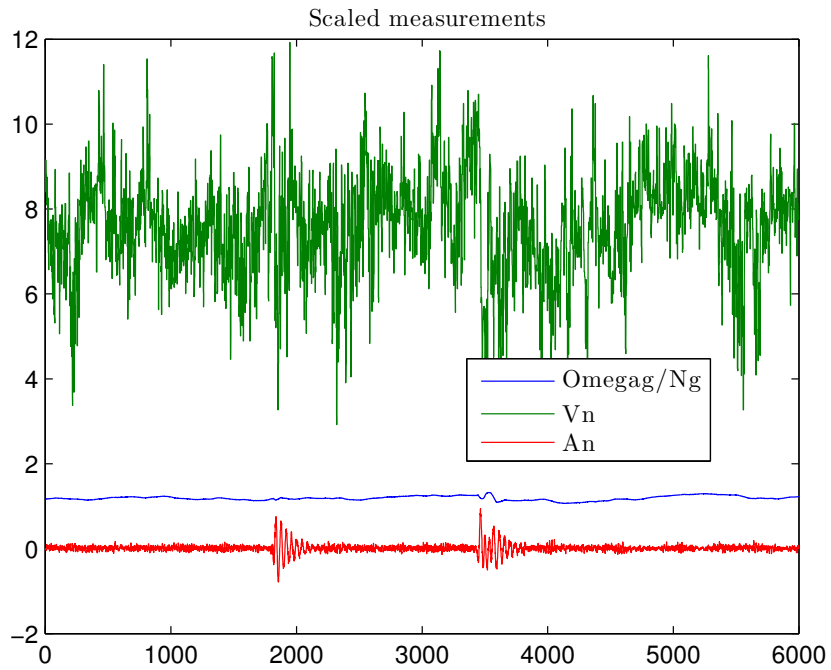


Figure 5.2: Measurements for full-scale test at mean wind below rated.

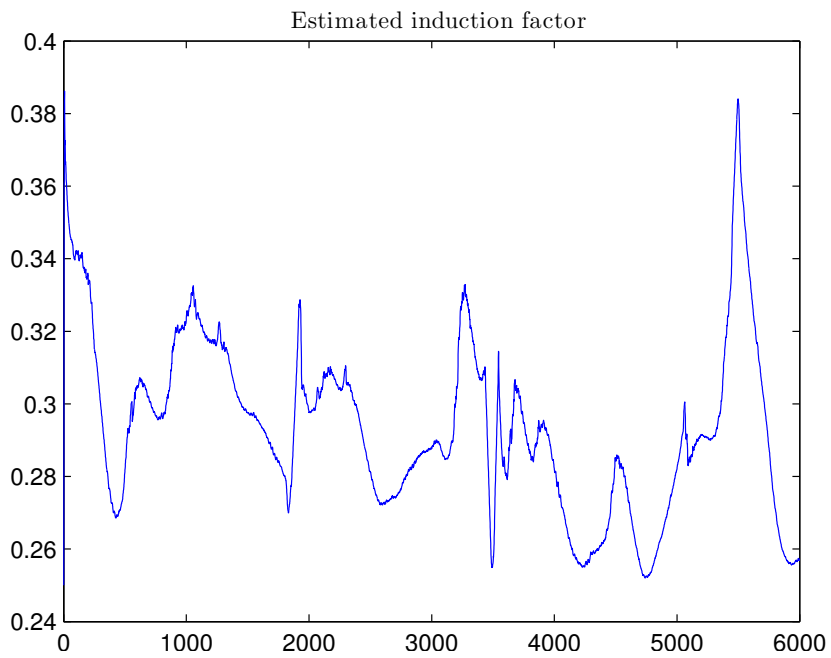


Figure 5.3: Induction factor estimate for full-scale test at mean wind below rated.

residual has peaks at the 3P the DT and then to frequencies in between. The first three peaks are at unmodeled dynamics namely the 3P and then perhaps some blade frequencies. As these are unmodeled this is to be expected. However, the DT peak should not be there as the DT is included in the model. Similarly for the acceleration residual, the small peak at the FT is not expected.

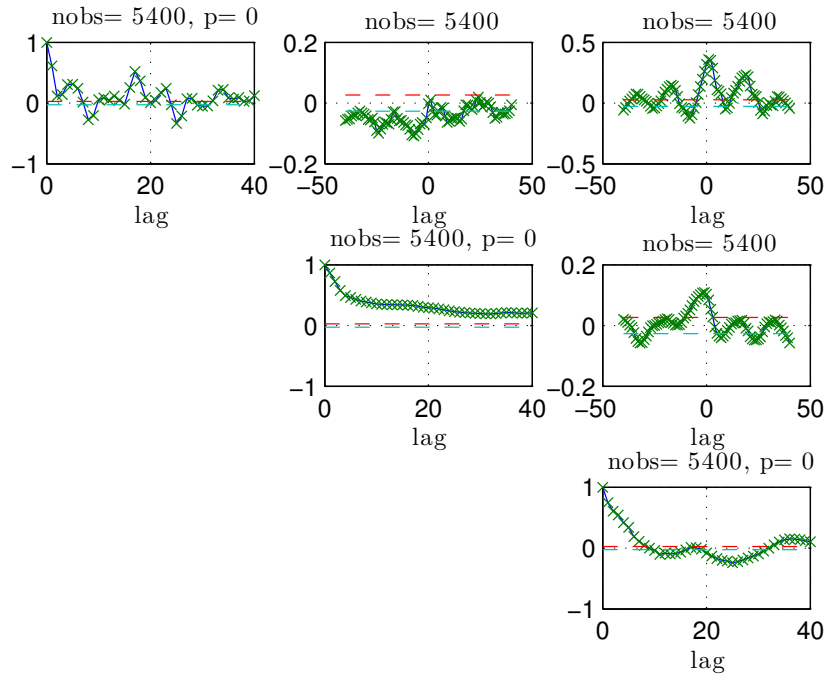


Figure 5.4: Residual test for the full-scale test at mean wind below rated.

5.4 Close to rated wind

The next data is close to rated wind speed as seen in figure 5.6 where the pitch is active all the time and there is also two time intervals from 300–400 sec. and from 550–600 sec. where the turbine is in pitch speed control operation mode. Again the estimated induction factor in figure 5.8 is hard to verify but at least it is low when the pitch is high.

Again the residuals are far from white as seen in figure 5.9–5.10. The wind measurements residual is again mostly of low pass type. The peaks from 3P and above which were seen in low wind are also seen here. The FT and 1P frequencies almost coincides for this wind speed. This means that the 1P probably gives sideways tower movements which can affect the generator speed measurements which again might carry over to the pitch via the speed controller. The unmodeled 1P disturbance in the generator speed can also simply spread via the Kalman gain to the other state estimates. This is a possible explanation for the large peak at FT/1P for both the speed and acceleration measurements. Then there is also a slower frequency peak around 0.2 which is difficult to explain.

Changing the covariances in the KF will change the behavior and potentially improve the performance. There is to many parameters to use trial and error approach for all of them. Therefore the rationale used is

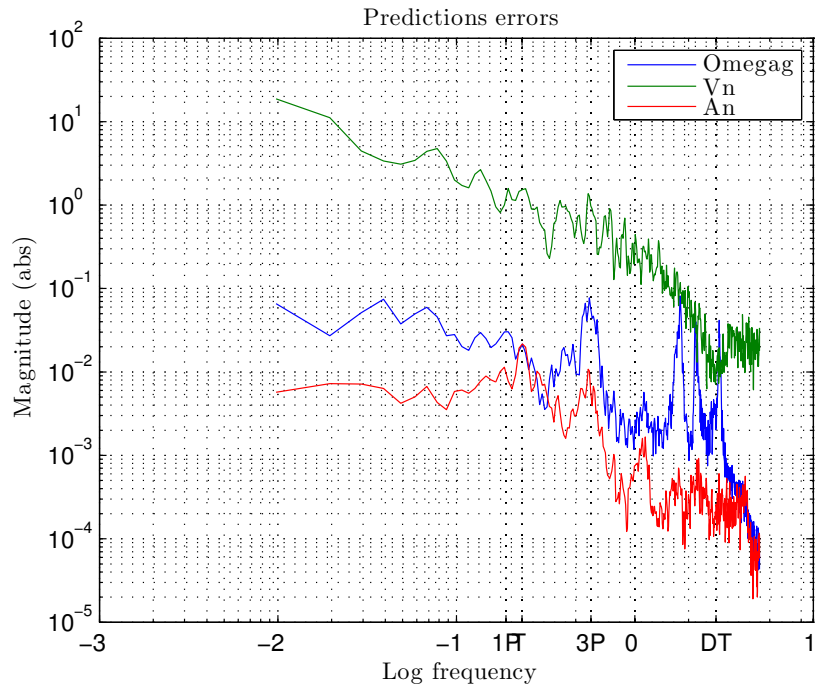


Figure 5.5: Residual spectrum for the full-scale test at mean wind below rated. Notice the extra tick marks for 1P, first tower (FT), 3P and drive train (DT) frequencies. 1P and FT are close together.

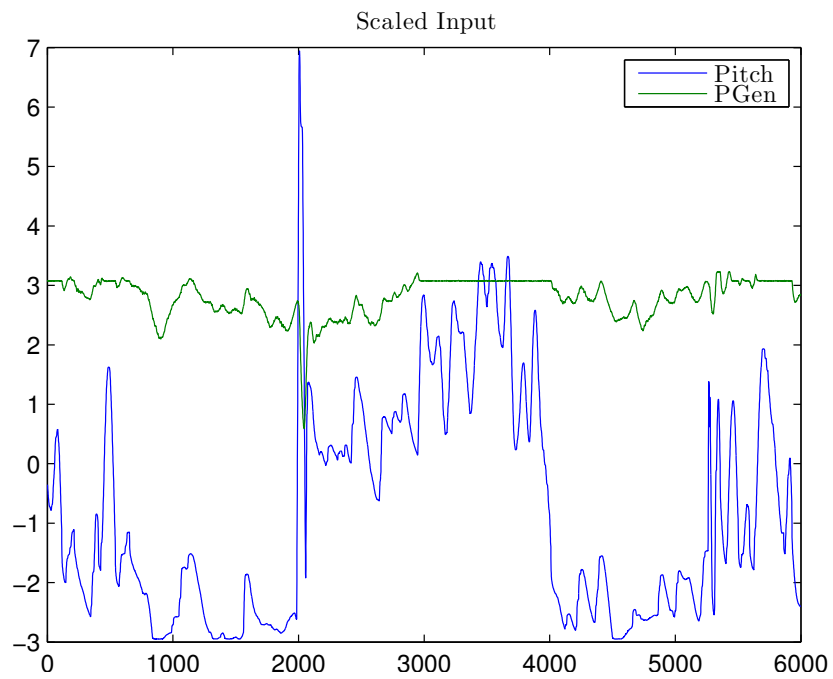


Figure 5.6: Input for full-scale test at mean wind close to rated.

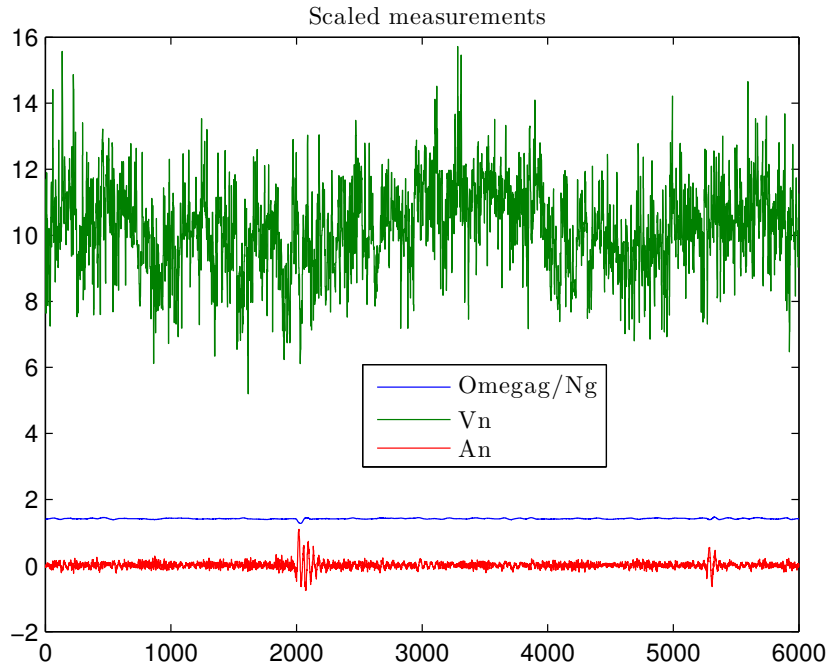


Figure 5.7: Measurements for full-scale test at mean wind close to rated.



Figure 5.8: Induction factor estimate for full-scale test at mean wind close to rated.

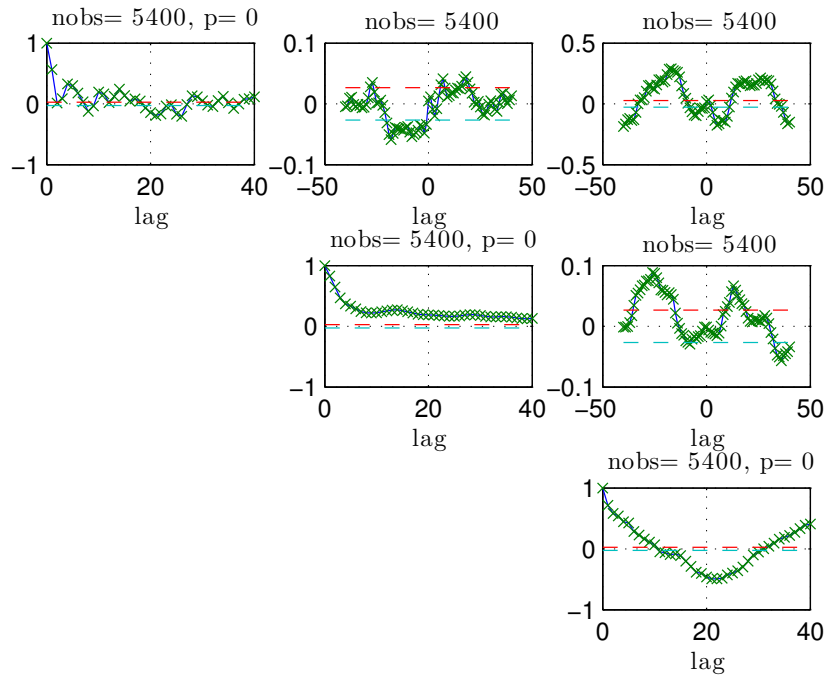


Figure 5.9: Residual test for the full-scale test at mean wind close to rated.

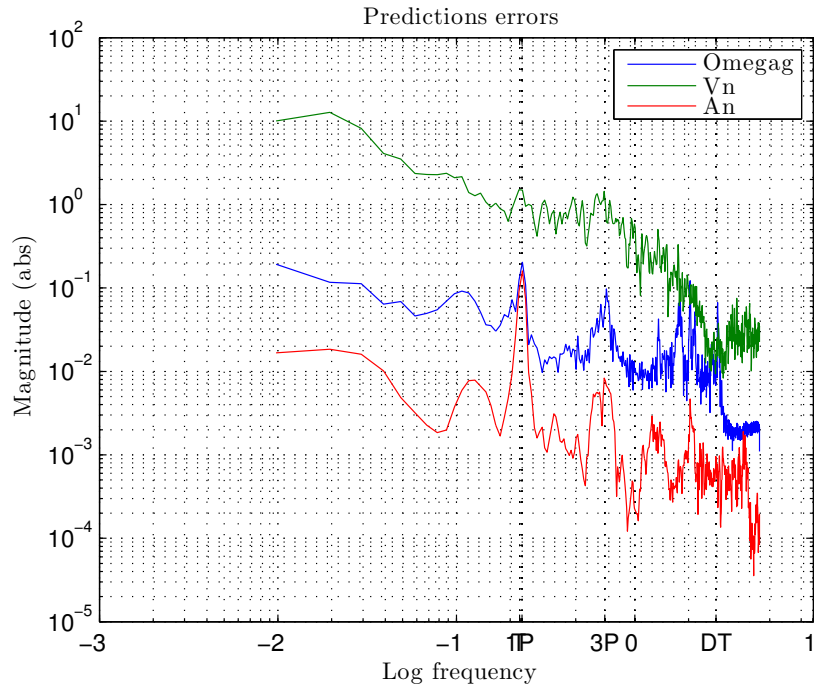


Figure 5.10: Residual spectrum for the full-scale test at mean wind close to rated. Notice the extra tick marks for 1P, first tower (FT), 3P and drive train (DT) frequencies. 1P and FT are close together.

to keep the process noise, i.e. wind part, covariances fixed. Also the measurements covariance for nacelle wind speed and acceleration has mostly been fixed. The generator speed measurements are considered as the prime measurement with the highest quality. If the speed covariance is increased compared to the above results the residuals spectrum peaks reduces but becomes more low frequent and larger. If it is decreased especially the 3P peak increases and also divergence can occur.

5.5 Discussion

It has not so far been possible to point to a few specific reasons for the non white residuals. There are at least the following many possibilities.

- The non-linearities are to large for the UKF to work. This is probably not very lightly.
- Problems with the parameters
 - C_p and C_t tables are with a perhaps to crude resolution which is 2 degrees for pitch and 0.5 for tip speed ratios. E.g. 0.5 for pitch and 0.1 for tip speed ratios would be better.
 - Tower frequency has already been corrected.
 - Rotor and generator inertia and similar "physical" parameters should be correct as they are not to difficult to measure/calculate.
- Problems with the current model structure.
 - The dynamic inflow part may not match reality.
 - The rest is very standard.
- Importance of what is left out from the model
 - 3P is clearly given errors when covariance on generator speed measurement is small.
 - Variations in efficiency for gear and generator and especially air density will be significant. When power, pitch and speed are considered very accurate then this unmodeled uncertainty ends up in the wind state. However, the relative error in wind speed will be approximately $1/3$ of the error in power e.g. for 25% error $\sqrt[3]{1.25} = 1.077$.
NREL Investigation: For NREL 5MW the effect of 10% to high air density has been tested. This increases the predicted state error rms by a factor of 3 for tower movement and 16 for the induction state while the other states where not affected. Notice that for both states the error is entirely a offset so maybe it is not to important for fatigue and control. The effect of 10% to low air density is similar.
 - Blades are not in the model. This is maybe why there is 3 peaks in the spectra for the generator speed at approximately 2, 2.1 and 3. The blade frequencies are presently unknown.
- Problems with low observability which maybe also present in the NREL 5MW test in section 4. This is considered to be a less significant problem compared to the above.

Further work based on the above could be.

- Improve resolution of C_p and C_t tables.
- Check other parameters once more.

- Use the un-transformed wind speed measurement.
- Include 1P and 3P effects in the model.
- Low pass filter measurement with cut off frequency close to 2 to get rid of higher order unmodeled dynamics from blades etc.
- Include a state for estimating air density or “total efficiency” and perhaps also
- Include measurement uncertainty for pitch and power.
- Investigate problems with colored residuals in the simulated case when the feedback is active.

Chapter 6

Conclusion

The main objective with this project is to test if a simple dynamic inflow model will improve the state estimation for a real commercial wind turbine. For this a successful development and test of a continuous discrete version of the unscented Kalman filter has been developed and tested. Test based on simulations using NREL5MW virtual turbine was also successful with no or low pitch activity. For high winds with pitch activity all the time the whiteness and other performance of the UKF degraded compared to the ideal for linear systems. This has not been explained so far. Test based on data from a real turbine shows that the estimator works and gives reasonably estimates but the residuals are far from white and improvements should be pursued. A number of potential improvements are suggested. Unfortunately the project can not be continued as planned in 2014 do to administrative changes. Therefore a final conclusion can not be given.

Bibliography

- T. Burton, D. Sharpe, N. Jenkins, and E. Bossanyi. *Wind Energy Handbook*. John Wiley, 2008.
- S. J. Julier, J. K. Uhlmann, and H. F. Durrant-Whyte. A new approach for filtering nonlinear systems. In *ACC 1995, Seattle*, pages 1628–1632, 1995.
- T. Knudsen and T. Bak. Simple model for describing and estimating wind turbine dynamic inflow. In *2013 American Control Conference, June 17 - 19, Washington, DC.*, pages 640–646. AACC, IFAC, 2013.
- T. Knudsen, M. Soltani, and T. Bak. Prediction models for wind speed at turbine locations in a wind farm. *Wind Energy*, 14:877–894, 2011. Published online in Wiley Online Library (wileyonlinelibrary.com). DOI: 10.1002/we.491.
- I. Munteanu, A. I. Bratcu, N.-A. Cutululis, and E. Ceanga. *Optimal Control of Wind Energy Systems*. Springer, 2008.
- S. Thrun, W. Burgard, and D. Fox. *Probabilistic Robotics*. The MIT Press, 2006.

Appendix A

Measurement specifications

To estimate effective wind speed (EWS), at least generator speed, generator power and blade pitch are needed. This will only be sufficient for sampling and averaging times of more than 1 sec. For control relevant modelling with sampling of 0.1 sec. or less many more signals are needed to include the necessary dynamics.

The ideal measurements specifications are shown in table A.1. However, data that do not fully comply can still be very valuable. The specific turbine type and size and whether it is off or onshore have less priority as long as it is a pitch to feather type.

The most interesting operating condition is around rated power where the effect of dynamic inflow is most pronounced. It will be very valuable to have data with forced pitch excitation e.g. in square wave stepping signals of 1-3 degrees and with periods of 100-200 sec. This can be done without disturbing the wind turbine operation much just below rated power when the normal pitch controller is not active. In full load it is still possible to add a pitch disturbance but the full load pitch controller must then be allowed to remove this disturbance again. Another possibility will be to use power reference changes to induce the pitch changes when in full load operation.

General	Sample time:0.1 sec. Averaging time: samplingt time Date / Time stamp: absolute
Wind turbine	Electrical power produced Electrical power reference (if available) Status signal Blade pitch angles (3) Generator speed Rotor speed (if available) Wind speed at turbine Wind direction at turbine Nacelle direction Tower acceleration fore aft and sideways
Meteo mast (if available)	Wind speed at 0.5, 1 and 1.5 hub height Wind direction at hub height Temperature at 0.5, 1 and 1.5 hub height
Conditions	Forced pitch excitation in partial load if possible Four wind speeds: (1) near cut-in, (2) halfway nominal power, (3) near nominal power, (4) high wind speed
Misc	Several (10) sets per wind speed At least 10 min. of data per set preferable longer.

Table A.1: Measurement specification

Appendix B

Parameter specifications

To estimate EWS with fast sampling e.g. 0.1 sec. all the below parameters in table B.1 are necessary.

Aerodynamics	CP and CT tables for the hole operating range of pitch and tip speed ratio
Drive train	Slow side (rotor) inertia Fast side (generator) inertia Spring constant and damping coefficient or Eigen frequency and damping
Generator	Losses e.g. viscous damping coefficient and zero load losses
Tower	Total top inertia Spring constant and damping coefficient or Eigen frequency and damping

Table B.1: Turbine parameter specification

Appendix C

Second order statistics for $y = x^T x$ for x Gaussian

The objective in this section is to find a test case for testing the unscented transform in section 2.3 where the exact theoretical result is known even though the relation is non linear. This is possible for the above relation as demonstrated below.

Assume the n dimensional vector x is defined by: covariance

$$x \in N(\mu_x, C_x) \Rightarrow \text{(by definition)} E(x) = \mu_x, \text{Cov}(x) = C_x, x \text{ Gaussian.} \quad (\text{C.1})$$

The problem is then to find $E(y)$, $\text{Cov}(y)$, $\text{Cov}(y, x)$.

An more useful representation of x is:

$$x = \mu_x + C_x^{\frac{1}{2}} e, e \in N(\underline{0}, I) \quad (\text{C.2})$$

where

$$C_x^{\frac{1}{2}} = UL^{\frac{1}{2}}, U, L \text{ are eigen vector and value matrices} \Rightarrow \quad (\text{C.3})$$

$$C_x^{\frac{1}{2}} C_x^{\frac{1}{2}T} = UL^{\frac{1}{2}} (UL^{\frac{1}{2}})^T = UL^{\frac{1}{2}} L^{\frac{1}{2}} U^T = ULU^T = C_x, \quad (\text{C.4})$$

$$C_x^{\frac{1}{2}T} C_x^{\frac{1}{2}} = (UL^{\frac{1}{2}})^T UL^{\frac{1}{2}} = L^{\frac{1}{2}} U^T UL^{\frac{1}{2}} = L^{\frac{1}{2}} L^{\frac{1}{2}} = L \quad (\text{C.5})$$

Below the following facts about normalised Gaussian variables are used.

$$e \in N(\underline{0}, I) \Rightarrow \quad (\text{C.6})$$

$$E(e_i) = 0, E(e_i^2) = 1, E(e_i^3) = 0, E(e_i^4) = \text{Var}(e_i^2) + E(e_i^2)^2 = 2 + 1 = 3 \quad (\text{C.7})$$

The mean $E(y)$ can then be found as follows:

$$\begin{aligned}
E(y) &= E(x^T x) \\
&= E((\mu_x + C_x^{\frac{1}{2}} e)^T (\mu_x + C_x^{\frac{1}{2}} e)) \\
&= \mu_x^T \mu_x + E((C_x^{\frac{1}{2}} e)^T C_x^{\frac{1}{2}} e) \\
&= \mu_x^T \mu_x + E(e^T C_x^{\frac{1}{2} T} C_x^{\frac{1}{2}} e) \\
&= \mu_x^T \mu_x + E(e^T L e) \\
&= \mu_x^T \mu_x + \text{trace}(L) \\
&= \mu_x^T \mu_x + \text{trace}(C_x)
\end{aligned} \tag{C.8}$$

The cross covariance $\text{Cov}(y, x)$ is found in a similar way where we use $E(e) = \underline{0}$, $E(ee^T) = I$, $E(e^T A e e^T B) = \underline{0} \quad \forall A, B$.

$$\begin{aligned}
\text{Cov}(y, x) &= E((y - \mu_y)(x - \mu_x)^T) \\
&= E((x^T x - \mu_y)(C_x^{\frac{1}{2}} e)^T) \\
&= E((x^T x)(C_x^{\frac{1}{2}} e)^T) \\
&= E((\mu_x + C_x^{\frac{1}{2}} e)^T (\mu_x + C_x^{\frac{1}{2}} e)(C_x^{\frac{1}{2}} e)^T) \\
&= E\left(\left(\mu_x^T \mu_x + \mu_x^T C_x^{\frac{1}{2}} e + (C_x^{\frac{1}{2}} e)^T \mu_x + (C_x^{\frac{1}{2}} e)^T C_x^{\frac{1}{2}} e\right) (C_x^{\frac{1}{2}} e)^T\right) \\
&= E\left(\left(\mu_x^T C_x^{\frac{1}{2}} e + (C_x^{\frac{1}{2}} e)^T \mu_x\right) (C_x^{\frac{1}{2}} e)^T\right) \\
&= E\left(\left(2\mu_x^T C_x^{\frac{1}{2}} e\right) (C_x^{\frac{1}{2}} e)^T\right) \\
&= 2\mu_x^T C_x^{\frac{1}{2}} E(ee^T) C_x^{\frac{1}{2} T} \\
&= 2\mu_x^T C_x
\end{aligned} \tag{C.9}$$

Finally $E(y^2)$ is derived.

$$\begin{aligned}
E(y^2) &= E((x^T x)^2) \\
&= E\left(\left((\mu_x + C_x^{\frac{1}{2}} e)^T (\mu_x + C_x^{\frac{1}{2}} e)\right)^2\right) \\
&= E\left(\left(\mu_x^T \mu_x + \mu_x^T C_x^{\frac{1}{2}} e + (C_x^{\frac{1}{2}} e)^T \mu_x + (C_x^{\frac{1}{2}} e)^T C_x^{\frac{1}{2}} e\right)^2\right) \\
&= E\left(\left(\mu_x^T \mu_x + 2\mu_x^T C_x^{\frac{1}{2}} e + e^T L e\right)^2\right) \\
&= (\mu_x^T \mu_x)^2 + 2\mu_x^T \mu_x \text{trace}(L) + 4\mu_x^T C_x \mu_x + E((e^T L e)^2)
\end{aligned} \tag{C.10}$$

$$\begin{aligned}
\mathbb{E} \left((e^T L e)^2 \right) &= \mathbb{E} \left(\left(\sum_{i=1}^n l_i e_i^2 \right)^2 \right) \\
&= \mathbb{E} \left(\sum_{i=1}^n \sum_{j=1}^n l_i l_j e_i^2 e_j^2 \right) \\
&= 3 \sum_{i=1}^n l_i^2 + \sum_{i=1}^n \sum_{j \neq i}^n l_i l_j \\
&= 2 \sum_{i=1}^n l_i^2 + \sum_{i=1}^n \sum_{j=1}^n l_i l_j
\end{aligned} \tag{C.11}$$

The covariance, or variance as it is a scalar, for y is

$$\begin{aligned}
\text{Cov}(y) &= \text{Var}(y) = \mathbb{E}(y^2) - \mathbb{E}(y)^2 \\
&= (\mu_x^T \mu_x)^2 + 2\mu_x^T \mu_x \text{trace}(C_x) + 4\mu_x^T C_x \mu_x + 2 \sum_{i=1}^n l_i^2 + \sum_{i=1}^n \sum_{j=1}^n l_i l_j \\
&\quad - (\mu_x^T \mu_x + \text{trace}(C_x))^2 \\
&= 4\mu_x^T C_x \mu_x + 2 \sum_{i=1}^n l_i^2
\end{aligned} \tag{C.12}$$

Appendix D

Detailed dynamic model

The EKF is based on a state space model. For convenience all the needed equations are collected in (D.1) starting with the state dynamics and ending with the static relations. The extension compared to the model used in Knudsen and Bak [2013] are the use of two inertias for the drive train compared to one in the previous work. Please see Knudsen and Bak [2013] for more details.

$$I_r \dot{\omega}_r = T_r - k_d \dot{\phi} - d_d \dot{\phi}, \quad (\text{D.1a})$$

$$I_g \dot{\omega}_g = (k_d \dot{\phi} + d_d \dot{\phi}) \frac{1}{N} - T_g, \quad (\text{D.1b})$$

$$\dot{\phi} = \omega_r - \omega_g \frac{1}{N}, \quad (\text{D.1c})$$

$$M_n \ddot{d}_n = F_r - k_t d_n - d_t \dot{d}_n, \quad (\text{D.1d})$$

$$\dot{v}_t = -\gamma(v_m) v_t + n_1, \quad (\text{D.1e})$$

$$\dot{v}_m = n_2, \quad (\text{D.1f})$$

$$\dot{a}_f = \kappa(v_m)(a_s - a_f), \quad (\text{D.1g})$$

$$\kappa(v_m) = \frac{2v_m}{3D}, \quad (\text{D.1h})$$

$$\gamma(v_m) = \frac{\pi v_m}{2L}, \quad (\text{D.1i})$$

$$V_1(v_m) = \frac{\pi v_m^3 t_i^2}{L}, \quad (\text{D.1j})$$

$$v_r = v_t + v_m - \dot{d}_n, \quad (\text{D.1k})$$

$$v_f = v_r \frac{1 - a_f}{1 - a_s}, \quad (\text{D.1l})$$

$$a_s = \frac{1}{2} \left(1 - \sqrt{1 - C_t(\lambda, \beta)} \right), \quad (\text{D.1m})$$

$$T_r = \frac{1}{2} \rho v_f^3 A_r C_p(\lambda, \beta) \frac{1}{\omega_r}, \quad (\text{D.1n})$$

$$F_r = \frac{1}{2} \rho v_f^2 A_r C_t(\lambda, \beta), \quad (\text{D.1o})$$

$$\lambda = \frac{\omega_r R_r}{v_r}, \quad (\text{D.1p})$$

$$T_g = \frac{p}{\mu\omega_r} . \quad (\text{D.1q})$$

The mechanical part is quite standard and are discussed in several text books [Burton et al., 2008, Munteanu et al., 2008].

The wind model is important for the estimator and is not standard. It is however well described in Knudsen et al. [2011].

The DI inflow part (D.1g), (D.1l) and (D.1m) is new while the rest of the aerodynamics (D.1n)– (D.1p) is standard except that the fictive wind v_f is used for rotor torque and thrust.

The measurement part (D.2) simply adds white measurement noise to the rotor speed ω_r , the wind speed seen by the nacelle v_r and the nacelle acceleration a_n .

$$\omega_m = \omega_r + v_1 , \quad (\text{D.2a})$$

$$v_n = v_r + v_2 , \quad (\text{D.2b})$$

$$a_m = a_n + v_3 . \quad (\text{D.2c})$$

The state space model with state, input and output is given below in condensed form.

$$x = [\omega_r \ \omega_g \ \phi \ \dot{d}_n \ d_n \ v_t \ v_m \ a_f]^T , \quad (\text{D.3})$$

$$u = [\beta \ p]^T , \quad (\text{D.4})$$

$$y = [\omega_m \ v_n \ a_m]^T \quad (\text{D.5})$$